Module VI, Lecture 05: Nuclear Quadrupolar Interaction

Nuclei with spin greater than ½ have non-spherical charge distribution, and the resulting electric quadrupole moment can interact with the electric field gradient. Because the direction of nuclear quadrupole moment is rigidly connected to the direction of the spin, this electrostatic interaction also manifests itself as a spin interaction, which is effectively quadratic – the spin "interacts with itself":

$$\hat{H}_{\mathrm{Q}}=-\frac{eQ}{2I\left(2I-1\right)}\hat{\vec{L}}\cdot\mathbf{V}\cdot\hat{\vec{L}}\qquad\qquad V_{ij}=\frac{\partial E_i}{\partial x_j}=-\frac{\partial^2\varphi}{\partial x_i\partial x_j}$$

where Q is the quadrupole moment of the nucleus (a fundamental constant), I is the spin of the nucleus, $\vec{E}$ is the electric field vector and φ is the electrostatic potential. The isotropic component of the quadrupolar interaction is related via Poisson's equation to the charge density at the nucleus, which may be considerable:

$$\sum_k V_{kk}=\frac{\partial^2\varphi}{\partial x^2}+\frac{\partial^2\varphi}{\partial y^2}+\frac{\partial^2\varphi}{\partial z^2}=\Delta\varphi=4\pi\left[q_N-e\left|\psi\left(\vec{r}_{\mathrm{N}}\right)\right|^2\right],$$

but the corresponding contribution to the nuclear spin Hamiltonian is static:

$$\hat{L}_{\mathrm{X}}^2+\hat{L}_{\mathrm{Y}}^2+\hat{L}_{\mathrm{Z}}^2=\hat{L}^2=l\left(l+1\right)\hat{E}$$

and for that reason is commonly dropped from consideration, because it amounts to the overall energy shift of the entire spin system. Therefore, it is only the traceless part of $\hat{H}_{\mathrm{Q}}$ that does in practice influence spin dynamics.

The most popular parameterization is of the anisotropy-asymmetry type:

$$eq=V_{\mathrm{ZZ}}-V_{\mathrm{Iso}}=V_{\mathrm{ZZ}},\qquad\qquad \eta=\frac{V_{\mathrm{XX}}-V_{\mathrm{YY}}}{V_{\mathrm{ZZ}}}$$

Where, by convention, $\left|V_{\mathrm{ZZ}}\right|\geq\left|V_{\mathrm{XX}}\right|\geq\left|V_{\mathrm{YY}}\right|$. Note that the asymmetry parameter becomes numerically ill-defined as the interaction approaches isotropic or axial form – that is known as the "axis switching" problem. In the principal axis frame using the parameters introduced above, we have:

$$\hat{H}_{\mathrm{Q}}=-\frac{e^2qQ}{4I\left(2I-1\right)}\left[3\hat{I}_{\mathrm{Z}}^2-\hat{I}^2+\frac{\eta}{2}\left(\hat{I}_{\mathrm{X}}^2-\hat{I}_{\mathrm{Y}}^2\right)\right]$$

The spin-independent part of the prefactor in this equation is known as the quadrupole coupling constant: $C=e^2qQ/\hbar$.

The behaviour of integer and half-integer spins under the quadrupolar hamiltonian is qualitatively different. In the case of half-integer spins, the quadrupolar interaction does not appear in the first-order perturbation correction for the energy difference along the central transition:

$$\Delta E_{-1/2,1/2}^{(1)}=\left\langle S,\frac{1}{2}\middle|\hat{H}_{\mathrm{Q}}\middle|S,\frac{1}{2}\right\rangle-\left\langle S,-\frac{1}{2}\middle|\hat{H}_{\mathrm{Q}}\middle|S,-\frac{1}{2}\right\rangle=0$$

The central transition is therefore immune (to first order in perturbation theory) to the orientation dependence introduced by the quadrupolar interaction and the corresponding spectral line stays sharp. Integer spin nuclei do not have this luxury and do therefore always display a broad powder pattern.

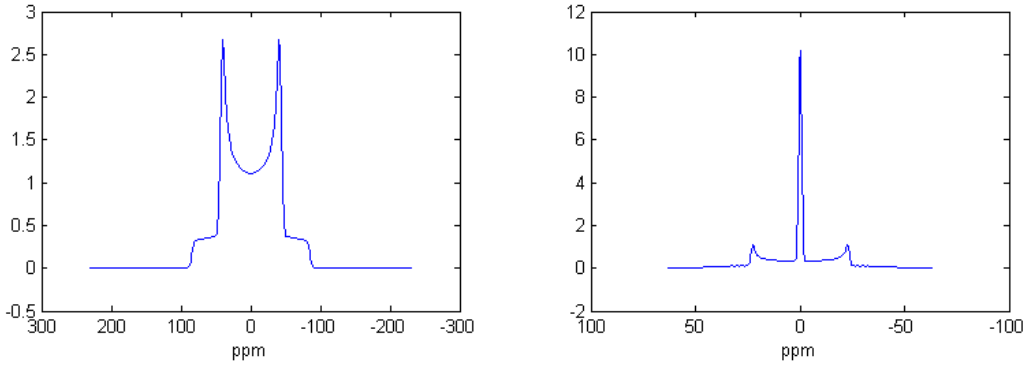

Fig 1. Quadrupolar powder patterns computed for ^{14}N (left) and ^{23}Na (right) nuclei with a small axial quadrupolar interaction. The sharp central transition is clearly visible for ^{23}Na.

The second-order perturbation theory correction for the central transition does have a quadrupolar contribution and therefore the central transition becomes less sharp (due to the orientation dependence appearing in $\Delta E^{(2)}_{-1/2,1/2}$) in systems where the quadrupole interaction is comparable in magnitude to Zeeman interaction with the applied magnetic field.

Quadrupolar interaction does not have rank-0 or rank-1 contributions and its irreducible spherical tensor form does therefore only have second rank components. In the principal axis frame:

$$\hat{H}_{\mathrm{Q}} = \frac{\sqrt{6}e^2qQ}{4I\left(2I-1\right)}\hat{T}^{(2)}_0 + \frac{e^2qQ\eta}{4I\left(2I-1\right)}\left[\hat{T}^{(2)}_{-2} + \hat{T}^{(2)}_2\right]$$

Rotations relative to the principal axis frame are applied using the standard spherical tensor relation:

$$\hat{\hat{R}}\left(\alpha,\beta,\gamma\right)\hat{T}^{(2)}_m = \sum_{m'=-2}^{2}\hat{T}^{(2)}_{m'}\mathfrak{D}^{(2)}_{m',m}\left(\alpha,\beta,\gamma\right)$$

Where the second rank spherical tensor operators for quadratic spin interactions are:

$$\hat{T}^{(2)}_{\pm 2} = \frac{1}{2}\hat{L}^2_{\pm}, \qquad \hat{T}^{(2)}_{\pm 1} = \mp\frac{1}{2}\left(\hat{L}_{\mathrm{Z}}\hat{L}_{\pm} + \hat{L}_{\pm}\hat{L}_{\mathrm{Z}}\right), \qquad \hat{T}^{(2)}_0 = \sqrt{\frac{2}{3}}\left(\hat{L}^2_{\mathrm{Z}} - \frac{1}{4}\left(\hat{L}_+\hat{L}_- + \hat{L}_-\hat{L}_+\right)\right)$$

and the Wigner functions $\mathfrak{D}^{(2)}_{m,n} = e^{-im\alpha}d^{(2)}_{m,n}\left(\beta\right)e^{-in\gamma}$ are tabulated below.

	$d^{(2)}_{m,2}$	$d^{(2)}_{m,1}$	$d^{(2)}_{m,0}$	$d^{(2)}_{m,-1}$	$d^{(2)}_{m,-2}$
$d^{(2)}_{2,n}$	$\frac{(1+\cos\beta)^2}{4}$	$-\frac{(1+\cos\beta)\sin\beta}{2}$	$\sqrt{\frac{3}{8}}\sin^2\beta$	$-\frac{(1-\cos\beta)\sin\beta}{2}$	$\frac{(1-\cos\beta)^2}{4}$
$d^{(2)}_{1,n}$	$\frac{(1+\cos\beta)\sin\beta}{2}$	$\frac{\cos\beta-1}{2}+\cos^2\beta$	$-\sqrt{\frac{3}{8}}\sin 2\beta$	$\frac{\cos\beta+1}{2}-\cos^2\beta$	$-\frac{(1-\cos\beta)\sin\beta}{2}$
$d^{(2)}_{0,n}$	$\sqrt{\frac{3}{8}}\sin^2\beta$	$\sqrt{\frac{3}{8}}\sin 2\beta$	$\frac{3\cos^2\beta-1}{2}$	$-\sqrt{\frac{3}{8}}\sin 2\beta$	$\sqrt{\frac{3}{8}}\sin^2\beta$
$d^{(2)}_{-1,n}$	$\frac{(1-\cos\beta)\sin\beta}{2}$	$\frac{\cos\beta+1}{2}-\cos^2\beta$	$\sqrt{\frac{3}{8}}\sin 2\beta$	$\frac{\cos\beta-1}{2}+\cos^2\beta$	$-\frac{(1+\cos\beta)\sin\beta}{2}$
$d^{(2)}_{-2,n}$	$\frac{(1-\cos\beta)^2}{4}$	$\frac{(1-\cos\beta)\sin\beta}{2}$	$\sqrt{\frac{3}{8}}\sin^2\beta$	$\frac{(1+\cos\beta)\sin\beta}{2}$	$\frac{(1+\cos\beta)^2}{4}$

It is in practice rarely necessary to type all this into a computer or work with explicit trigonometric represenations of Wigner functions – all of the functions and relations given above are already implemented into mainstream simulation software. *Mathematica 8.0* and above, in particular, would generate Wigner functions on demand.

Quadrupolar relaxation in liquid phase

Because quadrupolar interaction is traceless, it is averaged out in liquids by fast isotropic molecular rotation and only contributes indirectly to the relaxation processes. In non-viscous isotropic liquids at high magnetic field the contributions of quadrupolar processes to the relaxation rates are:

$$\frac{1}{T_1}=\frac{3}{20}\frac{(2I+3)C^2}{I^2(2I-1)}\left(1+\frac{\eta^2}{3}\right)\left[\frac{\tau_{\rm C}}{1+\omega_0^2\tau_{\rm C}^2}+\frac{4\tau_{\rm C}}{1+4\omega_0^2\tau_{\rm C}^2}\right]$$

$$\frac{1}{T_2}=\frac{3}{20}\frac{(2I+3)C^2}{I^2(2I-1)}\left(1+\frac{\eta^2}{3}\right)\left[9\tau_{\rm C}+\frac{15\tau_{\rm C}}{1+\omega_0^2\tau_{\rm C}^2}+\frac{6\tau_{\rm C}}{1+4\omega_0^2\tau_{\rm C}^2}\right]$$

where, in addition to the symbols defined above, ω_0 is the nuclear Zeeman frequency and $\tau_{\rm C}$ is the rotational correlation time.

Quadrupolar coupling in the rotating frame

Quadrupolar interactions have electrostatic origin and can therefore be large – the rotating frame approximation must therefore take into account the fact that the $\left\|\omega_0\hat{L}_{\rm Z}\right\|\gg\left\|\hat{H}_{\rm Q}\right\|$ condition does not always hold. For the spherical tensor expansion of the quadrupolar Hamiltonian:

$$\hat{H}_{\rm Q}^{\rm R}(t)=e^{-i\omega_0\hat{L}_Z t}\hat{H}_{\rm Q}e^{+i\omega_0\hat{L}_Z t}=e^{-i\omega_0\hat{L}_Z t}\left[\sum_{m=-2}^{2}q_m^{(2)}\hat{T}_m^{(2)}\right]e^{+i\omega_0\hat{L}_Z t}=$$

$$=\sum_{m=-2}^{2}q_m^{(2)}\left[e^{-i\omega_0\hat{L}_Z t}\hat{T}_m^{(2)}e^{+i\omega_0\hat{L}_Z t}\right]=\sum_{m=-2}^{2}q_m^{(2)}e^{-im\omega_0 t}\hat{T}_m^{(2)}$$

To the zeroth order in the average Hamiltonian theory, only one second rank term survives:

$$\left\langle\hat{H}_{\rm Q}^{\rm R}\right\rangle_0\approx\frac{\omega_0}{2\pi}\int_0^{2\pi/\omega_0}\hat{H}_{\rm Q}^{\rm R}(t)\,dt=\ldots=q_0^{(2)}\hat{T}_0^{(2)}$$

The first order term, however:

$$\left\langle\hat{H}_{\rm Q}^{\rm R}\right\rangle_1\approx-i\frac{\omega_0}{4\pi}\int_0^{2\pi/\omega_0}\int_0^{t}\left[\hat{H}_{\rm Q}^{\rm R}(t),\hat{H}_{\rm Q}^{\rm R}(t')\right]dt'dt=\ldots=-\frac{i\pi}{2\omega_0}\sum_{m=-2}^{2}q_{-m}^{(2)}q_m^{(2)}\left[\hat{T}_{-m}^{(2)},\hat{T}_m^{(2)}\right]$$

has contributions from spherical tensors operators up to $\hat{T}_0^{(3)}$ and Wigner functions up to $\mathfrak{D}_{m,n}^{(4)}$. In situations where the first-order term is significant, this complicates the experiments because the fourth-rank Wigner functions survive the traditional 54.73° magic angle spinning.

Quadrupolar coupling under MAS

Using standard pertrubation theory arguments for the rotating frame transformation with respect to the Zeeman Hamiltonian $\hat{H}_0=\omega_0\hat{L}_{\rm Z}$, we get the following frequency for the central transition:

$$\omega_{-1/2,1/2}=\left(\frac{e^2qQ}{4I(2I-1)}\right)^2\frac{3-4I(I+1)}{\omega_0}\left[(rank\ 0)+(rank\ 2)+(rank\ 4)\right]$$

where the terms in brackets are rather large and only their spherical tensor rank has been indicated. The primary difficulty stems from the presence of the fourth-rank terms in this expression – they transform under the fourth-rank Wigner functions that do not average to zero under magic angle spinning, meaning that MAS spectra of systems with large quadrupolar interactions are still broad.

One way around this problem is the double rotation (DOR) technique – sample is spun at two angles (magic angle and either 30.6° or 70.1°) simultaneously. The second angle corresponds to the roots of $\mathfrak{D}^{(4)}_{0,0}$ Wigner function:

$$\mathfrak{D}^{(4)}_{0,0}(\alpha,\beta,\gamma)=\frac{1}{8}\left(35\cos^4\beta-30\cos^2\beta+3\right)$$

and acts to average it out. The DOR technique is very challenging on the instrumental side – it involves one rotor spinning inside another at a considerable (upwards of a kHz) frequency.

Fig 2. DOR probe from David Bryce (University of Ottawa, Canada).

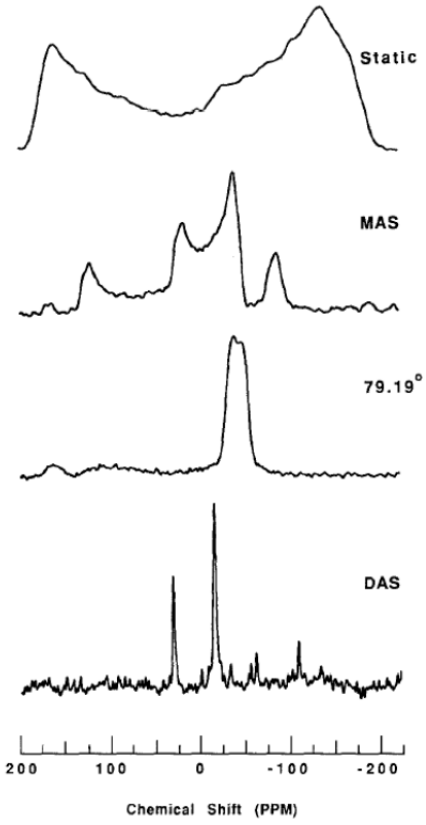

Fig 3. ^{17}O NMR spectra of cristobalite from the 1990 JMR paper by Alex Pines group.

Another way, called Dynamic Angle Spinning (DAS), uses a single spinning angle, but changes it as the experiment proceeds in such a way as to compensate the effects of the second- and fourth-order terms. In practice, the system is allowed to evolve for a period of time at a specific spinning angle θ_1, then the rotation axis is flipped to a different angle θ_2 and the system is allowed to evolve for a pre-calculated refocussing time, which is a function of the two angles. At the end of that time, the second and fourth rank terms are refocussed and only the isotropic contribution effectively remains. The echo time is then incremented in the indirect dimension. The magnetizaton can either be sampled at the echo maximum (producing a 1D NMR trace) or at all points after the echo maximum, producing a 2D spectrum with broad powder patterns in the direct dimension and sharp isotropic lines in the indirect dimension.

Both DOR and DAS have the disadvantage of requiring dedicated hardware. Only magic angle spinning hardware is available commercially however, and it is therefore advisable to find a technique that would only use spinning at the magic angle. Such a technique was developed by Lucio Frydman and co-workers; it became known as Multiple Quantum Magic Angle Spinning (MQMAS). It is conceptually similar to DAS, but the refocussing is achieved by switching the coherence order of the evolving magnetization rather than the Hamiltonian. The first sequence block is used to excite multiple-quantum coherence, which is evolved for a time t_1, then converted into a single-quantum coherence, which exhibits a spin echo after a predictable period of time kt_1. This echo signal is recorded and the evolution period t_1 is ioncremented in the indirect dimension. The result (1D or 2D spectrum, depending on the acquisition mode) is very similar to DAS. The

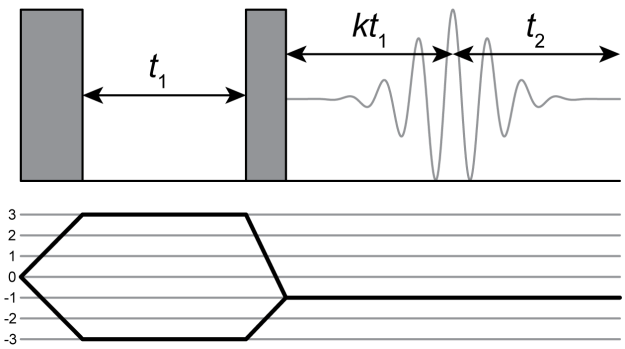

Fig 4. Block schematic of the MQMAS pulse sequence.

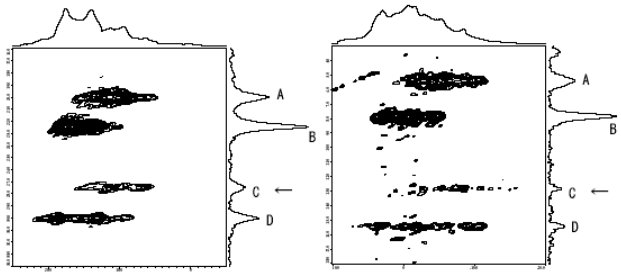

Fig 5. ^{23}Na 2D MQMAS example from JEOL Corporation.

coherence order selection and transfer is achieved by implementing a suitable phase cycle. The duration of the echo onset time relative to the t_1 evolution period depends on the initial level of the multiple-quantum coherence – tables may be found in the original literature.

Literature

1. L. Frydman, J.S. Harwood, *J. Am. Chem. Soc.*, **1995** 117 5367-5368.
2. K.T Müller, B.Q. Sun, G.C. Chingas, J.W. Zwanziger, T. Terao, A. Pines, *J. Magn. Res.*, **1990** 86 470-487.
3. I.P. Gerothanassis, C.G. Tsanaktsidis, *Conc. Magn. Reson.*, **1996** 8 63-74.
4. M.J. Duer, *Introduction to Solid-State NMR Spectroscopy*, Blackwell, 2004.